# PROSPECTS OF MULTI-GNSS TRACKING FOR FORMATION FLYING IN HIGHLY ELLIPTICAL EARTH ORBITS

**Erin Kahr**[(1)]
[(1)]*Department of Geomatics Engineering, Schulich School of Engineering, University of Calgary, 2500 University Drive NW, T2N 1N4, phone 1 403 210 9798, erinkahr@hotmail.com*

***Abstract:*** *Two formation flying missions are currently planned for highly elliptical orbit, NASA's Magnetosphere Multi Scale Mission and ESA's Proba-3; however, neither of these missions will take advantage of the new positioning opportunities offered by multi-constellation GNSS and their modernized signal structures. This paper investigates the potential benefits through a detailed visibility simulation which includes GPS, Galileo, GLONASS, BeiDou, QZSS, WAAS, EGNOS, GAGAN, SDCM and MSAS.*

*Results based on the Proba-3 orbit demonstrate that the GNSS signals are marginally detectable by a standard GNSS receiver, and therefore the output of any visibility simulation is highly dependent on the input simulation parameters. Because small changes to the mission and receiver or unexpected GNSS signal levels can significantly impact the visibility, investing in weak tracking and multi-constellation GNSS is particularly advantageous to mitigate the impact of uncertainty in the HEO environment. Under the right conditions, regional systems are shown to be particularly advantageous.*

***Keywords:*** *Multi-constellation GNSS, Differential GNSS, HEO, Proba-3*

## 1. Introduction

Formation flying in highly elliptical orbit around the Earth (HEO) offers numerous prospects for scientific research and technology demonstration. Aside from various studies and mission proposals made over the past decade, two actual HEO formation flying missions are currently under development. NASA's Magnetospheric Multiscale Mission (MMS) aims at a study of the Earth magnetosphere using a formation of four spacecraft, while the European Space Agency's Project for Onboard Autonomy 3 (PROBA-3) will study the Sun with a large coronagraph formed by two spacecraft in a tightly controlled formation. Both missions consider GPS as a sole or complementary navigation system to operate and control the formation. MMS will make use of GPS L1 C/A-code measurements as the only source of navigation information, and will meet the relative positioning accuracy requirement of 100m (at the most stringent) by post-processing the measurements on the ground [1,2]. Proba-3 will make use of GPS during the perigee passage and for coarse formation acquisition, while relying on optical positioning sensors for relative positioning at apogee when spacecraft alignment at the mm level will be required to achieve the scientific objectives [3,4].

Other than existing formations (GRACE, PRISMA, or TanDEM-X) in low Earth orbit (LEO), HEO missions no longer operate in the standard GPS Service Volume, which is confined to the near-Earth environment. Positioning outside the Service Volume is challenging because the GPS satellites have directive antennas which point towards the

Earth. There is some spill-over which allows satellites in LEO to have similar operating conditions to those on the Earth's surface, but receivers above the GPS satellites rely on positioning signals from the far side of the Earth, which results in poorer positioning geometry and weaker signals due to additional free-space path loss. Because the Earth obstructs a significant portion of the GPS constellations, it is also unlikely that the required number of GPS signals for single point positioning can be simultaneously tracked at high altitudes above the Earth. Figure 1 depicts the typical geometry of a Proba-3 type orbit and the GPS orbit. The blue line represents the approximate boundary of the area within which the GPS signal is strong enough to be acquired, assuming a 33 dB Hz acquisition threshold and a 3 dB isotropic receiving antenna.

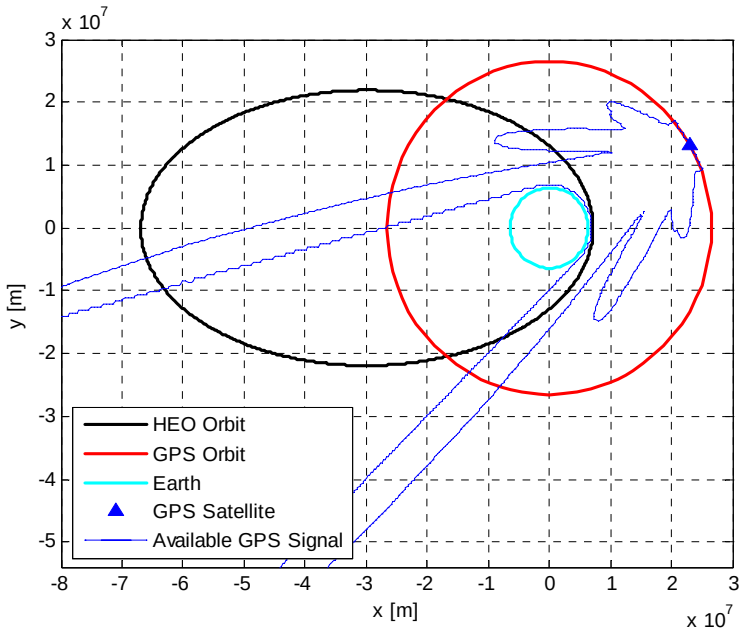


**Figure 1: Visibility of a GPS satellite from HEO**

Neither of the above mentioned HEO formation flying missions plans to take advantage of the new developments in Global Navigation Satellite Systems (GNSS), such as multiple constellations and new signal structures, for positioning outside the Service Volume. The new GNSS systems and modernized signal structures offer exciting advantages over legacy GPS. Among them are data and pilot channels which allow for longer coherent integration times to track weaker signals, wider signal bandwidths which potentially allow for more accurate code measurements, more frequencies which stand to improve the chances of carrier phase ambiguity resolution through wide-lane combinations, and most importantly an increased number of GNSS satellites, which substantially increases the number of simultaneous positioning measurements available to receivers outside the main GNSS service volumes. On the other hand, the new GNSS signals are more difficult to acquire, and there are system dependencies such as timing biases which must be properly accounted for in order to simultaneously use signals from different GNSS systems.

This paper presents insights into the advantages of using multi-constellation GNSS for HEO formation flying, based on a detailed visibility simulation. It builds on similar studies by [5-8] by discussing aspects such as the sensitivity of the visibility simulation to poorly known simulation parameters, the required number of satellites to obtain position updates under various conditions, the advantages of new signal structures for weak tracking, and the advantages and disadvantages of regional systems and satellite based augmentation systems.

The second section of this paper provides an overview of the simulation parameters describing the formation flying mission, the GNSS constellations, and the GNSS receiver characteristics. The third section presents the results from various simulations, and the fourth section summarizes the conclusions.

## 2. Simulation and Assumptions

In order to assess the value of the various GNSS constellations, a detailed visibility simulation tool was created to calculate the geometry and link budgets of the GNSS constellations relative to a receiver on a user defined satellite. A goal of the visibility simulation was to have the software remain as flexible as possible, in order to easily change any element of the simulation. In the process of building the simulation a vast number of assumptions therefore had to be made and justified in order to obtain results: assumptions about the formation flying mission, about the GNSS constellations, and about the GNSS receivers.

### 2.1 Formation Flying Mission

The results presented in this paper are based on a Proba-3 type formation flying mission. Table 1 summarizes the assumed orbital elements, which are based off of [9] and the same as those used for the study in [10].

**Table 1: HEO Orbital Parameters**

| ***Element*** | ***Value*** | ***Units*** |
|---|---|---|
| a | 37039887 | metres |
| e | 0.80620521 | |
| i | 59 | degrees |
| $\omega$ | 187 | degrees |
| $\Omega$ | 142 | degrees |
| $\nu$ | 0 | degrees |
| GM | 3.98601E+14 | $m^3/s^2$ |

In carrying out the research two attitude profiles were assumed. The first is an “ideal” inertial profile with the GNSS antenna oriented parallel to the line of apsides towards perigee, which was found to be nearly optimal in terms of number of visible GNSS satellites throughout the orbit, and optimal in terms of both simplicity and in terms of the mean tracking arc duration through the perigee passage. It is depicted in Figure 2. The majority of the presented results are for this case.

The second attitude profile is a sun-pointing profile, in keeping with the Proba-3 mission requirements. It makes the assumption that the GNSS antenna is on a face orthogonal to the sun pointing vector, and is therefore able to freely rotate about the sun vector such that the antenna boresight is as closely aligned with the ideal profile as possible. The sun pointing profile introduces a time of year dependence into the results, with two optimal dates in mid-May and mid-November when the sun vector is normal to the orbital plane and the sun-pointing profile reduces to the ideal profile, and two critical dates in mid-February and mid-August when the sun is aligned with perigee and apogee respectively, and the antenna is forced to point perpendicular to the ideal case.

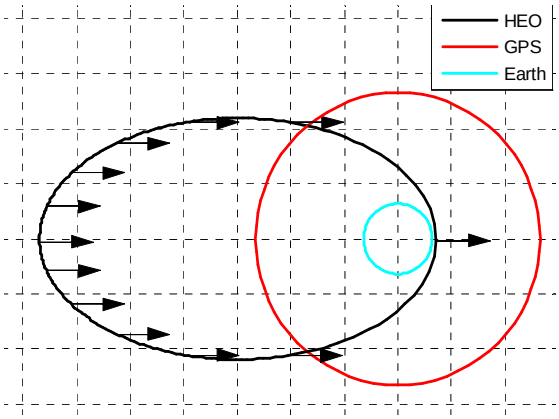


**Figure 2: Ideal attitude profile for HEO GNSS tracking**

## 2.2 GNSS Constellations and Signals

Six sources of satellite navigation messages have been considered in this study: GPS, GLONASS, Galileo, BeiDou, QZSS and the satellite based augmentation systems (SBAS).

*GPS*

GPS is the fully operational American GNSS, consisting of a minimum of 24 active satellites in six orbital planes, with an orbital radius of approximately 26561 km. The GPS satellites historically transmit a civilian signal on the L1 frequency, and a precise military signal on the L2 frequency, but the system is being modernized to transmit a new signal on L1, a civilian L2 signal, as well as an L5, all of which have modernized signal structures for improved tracking accuracy and weak signal tracking [11-13]. GPS is the only system of the six for which tracking beyond the service volume has been demonstrated [14-16].

*GLONASS*

GLONASS is the fully operational Russian GNSS, consisting of 24 active satellites in three orbital planes with an orbital radius of 25478 km and currently transmitting legacy civilian signals on L1 and L2. GLONASS uses frequency division multiple access (FDMA) to distinguish between satellites, which adds an element of complexity as each satellite transmits at slightly different frequencies. Modernization plans include transmitting code division multiple access (CDMA) signals on L1, L2, L3 and L5. [17-19]

*Galileo*
Galileo is the European GNSS currently under development. The full system will consist of 27 satellites plus 3 active spares in 3 orbital planes with an orbital radius of 29601 km, four of which have been launched. Galileo will transmit E1, E5a and b, and E6 signals which all have modern signal structures for improved accuracy and weak tracking. E1 shares the same center frequency as GPS L1, and E5a as GPS L5 for improved compatibility [20].

*BeiDou*
BeiDou is the Chinese GNSS currently under development. It is being completed in two phases. The first is the regional system consisting of a combination of satellites, five in geostationary orbit (GEO), five in inclined geosynchronous orbit (IGSO), and four in medium earth orbit (MEO), which is fully operational as of late 2012. The second phase, consisting of a global system of MEO satellites, is expected to be operational by 2020. As of yet only the B1 I signal, which has a slightly different centre frequency than GPS L1 and Galileo E1, has been defined in the interface control document [21]. B2 and B3 signals, at the same frequency as Galileo E5b and nearly the same as Galileo E6, have also been observed and tracked [22,23].

*QZSS*
The Quazi-Zenith Satellite System (QZSS) is Japan's regional augmentation system which is currently under development. According to the current ICD it will consist of three inclined geosynchronous satellites (one is currently operating) in elliptical orbits such that they are at apogee over Japan, to supplement the other GNSS systems in Japan's urban canyons [24]. More recent information suggests that the final constellation will consist of four or seven satellites [25]. The QZSS system will transmit GPS L1C/A, L1C, L2C, L5, and L6 LEX signals as well as SBAS type corrections on L1 and future L5 for maximum compatibility.

*SBAS*
The satellite based augmentation systems (SBAS) typically consist of payloads on geostationary communications satellites re-transmitting information to aid GPS/GNSS positioning for users. The primary purposes of SBAS are to provide the aviation community with atmospheric corrections and better positioning integrity. There exist a number of systems, including the US WAAS [26], European EGNOS [27], Japanese MSAS, Russian SDCM, and Indian GAGAN, which consist of 1-3 satellites each. These satellites transmit on the L1 and sometimes L5 frequencies, but have a different clock concept than the true GNSS systems, with the result that the clock and orbit errors are not as well known.

*GNSS Constellation Assumptions*
The positions of the GNSS satellites have all been computed from two line element sets (TLEs) for January 14 and 15, 2013, and the simulations were carried out for same dates for a realistic alignment of the GNSS satellites. Only existing, operational GNSS satellites have been simulated with the exception of Galileo, in which case the TLE of

the existing four satellites were used as the starting point and modified to obtain TLEs for a full 27 satellite Walker constellation.

The design of the GNSS satellites, in terms of transmitting antenna gain pattern and equivalent isotropically radiated power (EIRP), makes a very significant difference in the signal strength at a given point in space, and therefore in the number of visible GNSS satellites. The assumed gain patterns are depicted in Figure 3.

The GPS pattern is an average of the four orientations of the Czopek pattern [28], which was found to agree well with all other alternatives found in literature [15,16,29,30].The GAGAN pattern was presented in [31], the Galileo pattern in [32], the centre of the QZSS pattern in [33] and the WAAS prototype in [34]. For lack of better information, the GLONASS and BeiDou MEO patterns are assumed to be the same as GPS with the side lobes removed. The WAAS prototype is used for all SBAS systems not otherwise specified, and the QZSS profile was assumed for the BeiDou IGSO/GEO satellites. Although there is known to be a strong azimuth dependence in the GNSS patterns, insufficient information is available to adequately model it, and instead all gain patterns are assumed to be radially symmetric. Block dependence is also ignored in all cases except to differentiate MEO and geosynchronous satellites for BeiDou.

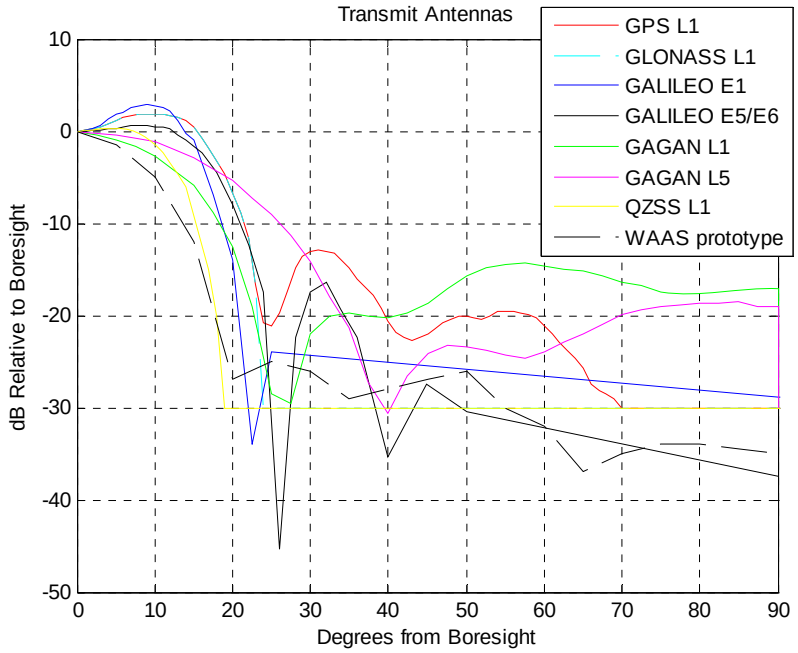


**Figure 3: Assumed transmission gain patterns for the GNSS systems**

The EIRP values were back calculated from the minimum received signal powers for a user on the earth and a GNSS satellite at 5 degree elevation (specified in the systems' ICD's), the transmission gain patterns, an assumed atmospheric loss of 2 dB on the earth, and a free space path loss calculated from the GNSS satellites' orbital altitudes. The signal power at an arbitrary point in the HEO orbit can then be calculated as in equation 1.

$$C\ (dBW) = EIRP\ (dBW) + G_{Tx}(dB) + L_{atm}(dB) + L_{path}(dB) \quad (1)$$

Where C is the signal power, $G_{Tx}$ is the transmit antenna gain in the direction of the point, $L_{atm}$ is the atmospheric loss assumed to be zero, and $L_{path}$ is the free space path loss. To compensate the assumption that atmospheric loss is zero in HEO, a 500 km mask of the earth was added to exclude signals passing through dense atmosphere near the earth's surface.

In spite of the efforts made to model them, transmission gain patterns and EIRP remain significant sources of uncertainty in any study of this type, and the results should therefore not be taken out of context.

### 2.3 GNSS Receiver Parameters

The choice of GNSS receiver has an impact of all aspects of the study. The behavior of a particular receiver is determined by the front end and the acquisition and tracking loop algorithms, which are built on may minor design decision which may even be unique to particular signals. These determine not only which signals and systems may be tracked, but also how whether the receiver is able to acquire and track a signal with a given received power. There are therefore an uncountable number of implicit assumptions built into any simulation of this type.

For the purposes of this study, the receiver behavior has been modeled by two numbers, the acquisition and tracking thresholds. All signals at or above the acquisition threshold are assumed to be instantaneously acquired, and it is assumed that lock is maintained until the signal drops below the tracking threshold. No consideration has been given to the time required for acquisition because it is expected to be on the order of a few minutes, insignificant given the simulation time step of 5 minutes. Unless otherwise stated, the results presented in this study were generated assuming using a common acquisition threshold for all signals and constellations of $C/N_0$ = 33 dB Hz and a tracking threshold of $C/N_0$ = 25 dB Hz.

The equation used to translate signal power at the receiving antenna to the carrier to noise density ratio, $C/N_0$, is equation 2 below.

$$C/N_0\ (dB\ Hz) = C\ (dBW) + G_{Rx}\ (dB) - (\ K_B\ (dBW/K\ Hz) + T_{sys}(dBK)) \quad (2)$$

Where C is the signal strength as defined in the previous section, $G_{Rx}$ is the receiving antenna gain in the direction of the GNSS satellite, $K_B$ is Boltzmann's constant, and $T_{sys}$ is the system noise temperature.

The $T_{sys}$ value is the sum of the sky/antenna temperature, $T_{sky}$, and the receiver noise temperature. The receiver noise temperature derives from a reference temperature $T_0$ as well as the noise figures, NF, losses, L, and gains, G, of the receiver front end. The equation for $T_{sys}$ is equation 3 below [35].

$$T_{sys} = T_{sky} + T_0\left[L_1 - 1 + L_1[NF_1 - 1 + G_1^{-1}[L_2 - 1...]]\right] \quad (3)$$

A “typical” value for $T_{sys}$ of 207 K = 23.2 dB K based on calculations in [36] has been used, which results in reasonable peak $C/N_0$ values on the order of 53 dB-Hz for a 3 dB RHCP hemispheric antenna on the earth’s surface. The reference temperature is assumed to be 290 K, as in [35]. However, according to the HEO specific link budget computations in [37], which use slightly different equations, it appears that $T_{sky}$ is neglected altogether and the reference temperature $T_0$ ranges from 180 K to 290 K depending on the antenna pointing direction. The difference in the two equations is on the order of 2 dB Hz, which is well within the level of uncertainty of the GNSS transmit gain patterns, but again highlights the extent to which the results should be taken in context.

Finally, the receiving antenna was assumed to be hemispheric, with the gain pattern of Figure 4, a hard cut off 85 degrees from bore sight, and a 3 dB peak gain.

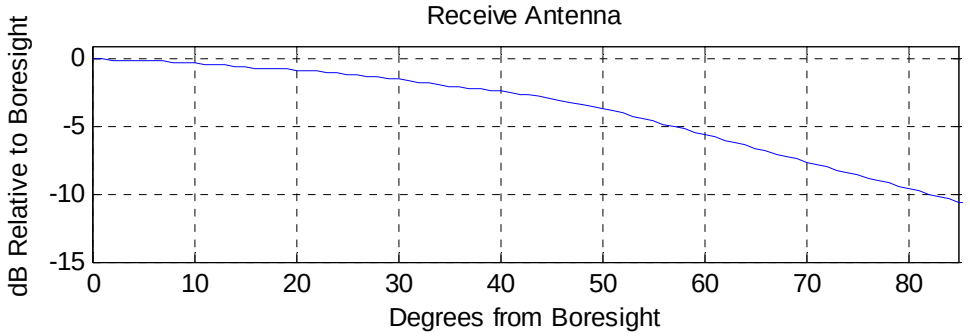


**Figure 4: Receiving Antenna Gain Pattern**

## 3. Results

Although a considerable number of cases have been tested in the simulation, a small subset of the results are presented which highlight the potential benefits of multiple MEO constellations, new signal structures, and regional systems.

The overarching assumption in the results is that the formation flying spacecraft share nearly identical attitude profiles, and therefore all visible GNSS satellites are common to all satellites in the formation.

### 3.1 Multiple MEO Constellations

For kinematic positioning, the number of unknowns using a single GNSS system is four, regardless of whether it is single point or relative kinematic positioning. Three of these unknowns are the 3D (relative) position components, and the fourth is the (relative) time offset. The time offset is of particular importance for relative positioning, because it allows the measurements from multiple receivers to be synchronized. At orbital velocity even a slight timing difference can lead to a large error in relative position. It is therefore a minimum requirement of kinematic positioning to simultaneously track four common GNSS satellites. More GNSS satellites well distributed in the sky provide more accurate positioning.

The right hand plot in Figure 5 depicts an example of the GPS only visibility from a highly elliptical Proba-3 type orbit over one period. The minimum kinematic positioning conditions are only met during the perigee passage at the beginning and end of the plot. However, knowledge of the orbital dynamics can also be used to supplement the GNSS measurements, so that even a single common GNSS satellite can be used to provide information about the relative clock offset. The timing accuracy in this case is only as good as the knowledge of the orbital position, where 1 ns = 30 cm. Additional measurements provide an update to the relative position estimate.

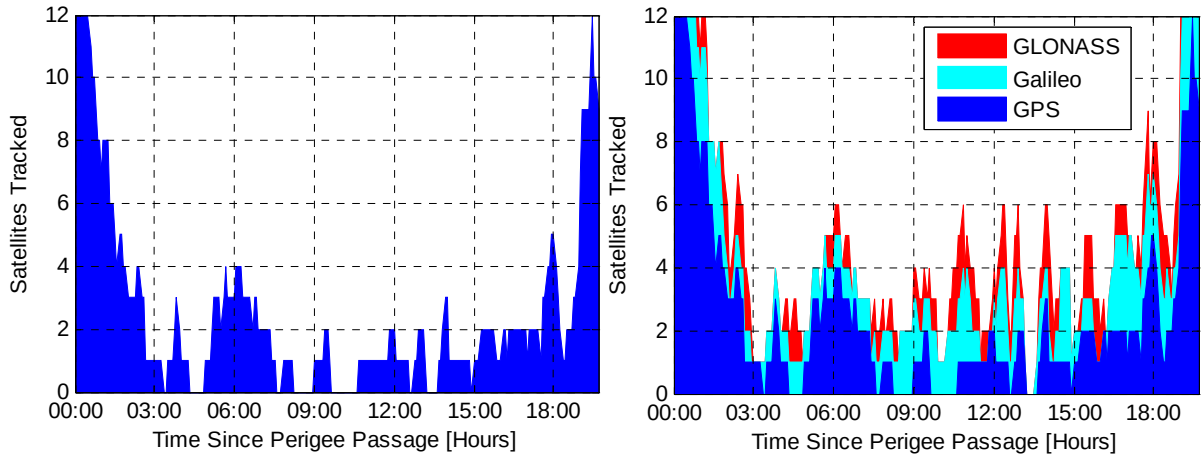


**Figure 5: Benefit of positioning with multiple MEO GNSS constellations**

The left hand plot in Figure 5 depicts the advantage of using three GNSS systems simultaneously. In this case an additional unknown is added for each new GNSS system, to account for inter-system timing biases caused by both signal-dependent receiver hardware delays and the different realizations of UTC that each system is referenced to. In spite of the additional unknowns, there is a clear advantage in terms of the number of tracked satellites using multiple GNSS systems. Take for example the spike in visibility 11 hours past perigee, when two GLONASS and three Galileo satellites are visible in addition to the one GPS satellite, briefly providing the necessary six measurements for resolution of the relative time, two inter-system biases, and three relative positioning coordinates.

These visibility results are highly dependent on the input assumptions about the formation flying orbit, antenna pointing profile, and alignment of the orbital planes. Tests with the sun-pointing profile around critical dates revealed that no satellites from any GNSS system are visible for several hours at apogee. Tests using different right ascension of the ascending node values for the FF orbit revealed a strong dependence on the alignment of the apogee with the GNSS orbital planes, which evolves over time. The effect is slightly more pronounces for Galileo and GLONASS's three orbital planes, as opposed to GPS's six. A test using a Molniya user orbit showed improved MEO visibility, as more GNSS orbital planes are grazing the earth from the Molniya satellite point of view and therefore more GNSS signals are strong enough to track.

### 3.2 Impact of New Signal Structures

The additional GNSS systems and modernized GNSS signals also offer advantages for weak tracking. In particular, many of the new signals have data and pilot components, which on one hand make for a higher combined signal strength, and on the other hand allow for improved weak tracking on the pilot signal because there are no unknown data bit transitions to interrupt tracking. Figure 6 shows the visibility of the Galileo E1 data/pilot signal based on tracking thresholds of 28 dB Hz for normal tracking vs. 20 dB Hz for a tracking algorithm taking advantage of the data/pilot signal structure. The tracking thresholds are based on [38].

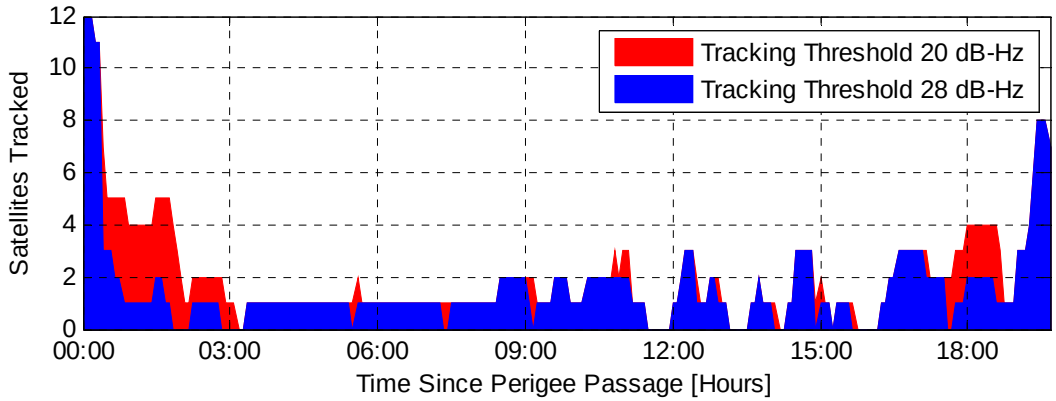


**Figure 6: Impact of a 20 dB-Hz vs. 28 dB-Hz tracking threshold on visibility**

The decreased tracking threshold has clear advantages, in particular for maintaining lock on side lobes of the GNSS signals when leaving or approaching perigee. At higher altitudes, the tracking arcs are extended by 5-10 minutes, bridging gaps and providing some overlap in tracked satellites for example in the period from 4 to 8 hours past perigee.

Other simulation parameters can be modified to achieve similar results. Lowering the acquisition threshold extends the tracking arcs as well, by allowing signal to be acquired earlier. Changing the assumed transmit pattern for the GNSS satellites can likewise increase or decrease the chances of acquiring side lobes and maintaining lock, as can raising or lowering the assumed EIRP or the receiver noise temperature. The sensitivity of the results to the input assumptions highlights the limited reliability of any study of this type, but also clearly demonstrates that investing in weak tracking is worthwhile as a means of mitigating the impact of unknown GNSS visibility.

### 3.3 Regional Systems

Neither QZSS nor the SBAS systems appear to have been considered for HEO positioning in previous studies, and until recently the BeiDou system suffered from a severe lack of publicly available information which made any sort of visibility assessment difficult. There are however several reasons these satellites are worth investigating.

First, they stand to provide a substantial improvement in geometry for a HEO satellite approaching or leaving perigee, when the GNSS satellites in MEO are only visible near the earth's limb but the SBAS/QZSS/BeiDou GEO/IGSO satellites are potentially still visible overhead. Second, they are characterized by a potentially higher transmit power focused into a narrower beam to compensate for their higher orbits, which is an advantage for tracking over the earth's limb but may also add to the "near-far" jamming problem. These factors are illustrated in Figure 7, which compares the visibility regions for the GPS, WAAS and GAGAN antenna patterns. The SDCM antennas additionally point 7 degrees northward for better coverage of the Russian territory, which also increases the amount of spill-over beyond the earth. Finally, the QZSS and SBAS satellites enjoy excellent compatibility with GPS in terms of the signal structures, which are identical for QZSS and nearly identical with a higher data rate for SBAS.

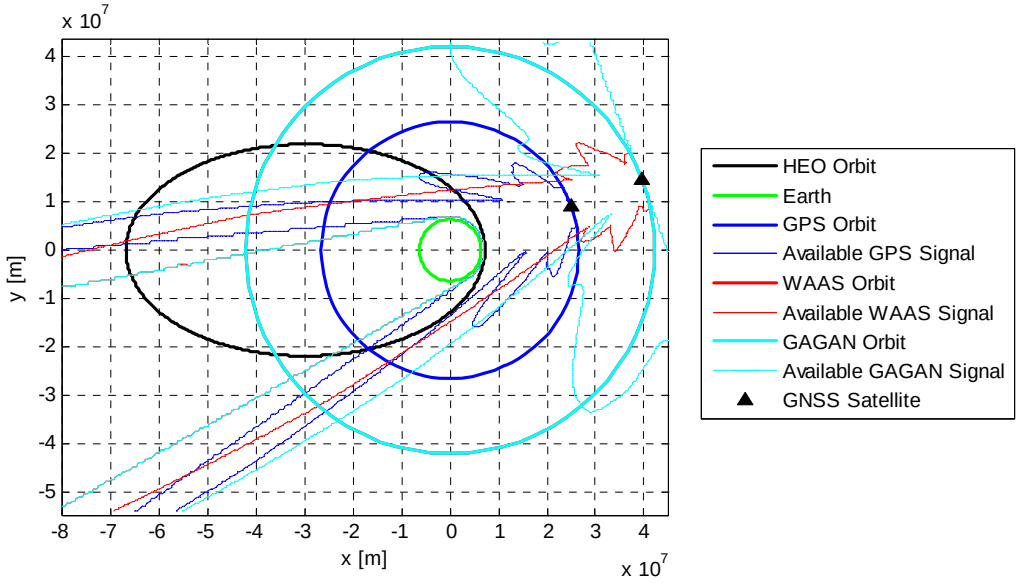


**Figure 7: Comparison of the GPS, WAAS and GAGAN visibility regions**

The potential disadvantages are that the intersystem biases are not well documented and may be substantial for a user so far outside the intended SBAS coverage regions. SBAS use a "bent pipe" approach rather than onboard atomic clocks, in which the signals are constantly monitored from the ground and adjusted to maintain accurate timing compared to GPS for a ground user in a specified coverage area [26]. Also, neither EGNOS nor SDCM is currently transmitting sufficiently accurate orbit data for navigation, and in general the SBAS orbits and clocks may be substantially less accurate than GPS. Finally, input parameters used in the link budget calculations for these systems are particularly poorly known, so the results are only a rough first approximation of what might be possible.

Nevertheless, as depicted in Figure 8 the results are quite optimistic. Nearly constant single satellite coverage of the Proba-3 orbit is achieved despite only one QZSS and 12 SBAS satellites being simulated, as compared to a 27 MEO satellite constellation. Occasional tracking of multiple satellites occurs, and the tracking arcs are longer than for the MEO satellites with less frequent loss of lock and acquisition. Because the SBAS

satellites are typically in geostationary orbits along the equator, the coverage is particularly good for the Proba-3 orbit but would be quite limited for a polar orbit.

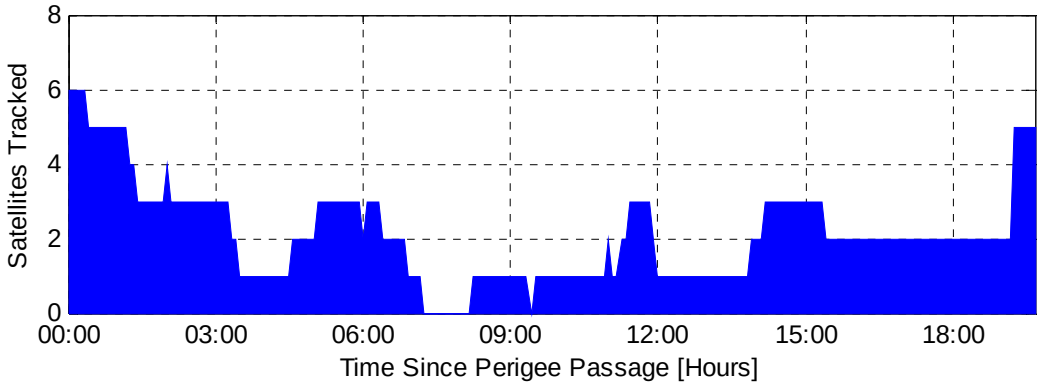


**Figure 8: Combined SBAS and QZSS visibility**

Even more interesting results are obtained for the regional BeiDou system, shown in Figure 9. Predictably, the visibility results vary dramatically depending on the alignment of the HEO and GNSS constellations. When the HEO apogee is opposite China (left) the visibility very nicely complements the MEO systems, with the best conditions occurring at or near apogee. On the contrary, when the apogee is over China (right) BeiDou contributes very little, with only brief tracking of the MEO satellites at apogee. While the time of day dependence reduces the usefulness of BeiDou for a 20 hour orbit, a properly aligned HEO mission with a 24 hour orbital period or a mission in geosynchronous orbit could experience a substantial benefit.

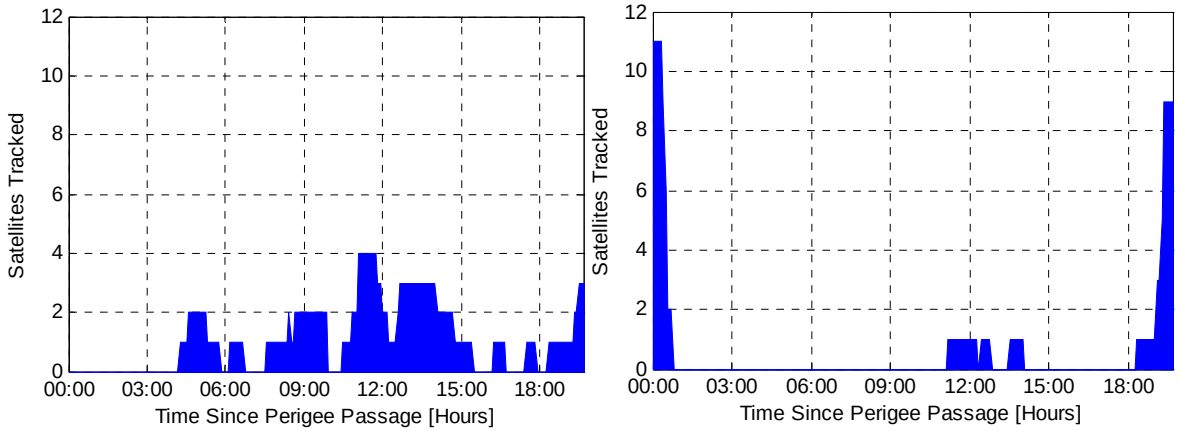


**Figure 9: Visibility of the BeiDou regional system from HEO. Left: apogee opposite China, right: apogee over China**

## 4. Conclusions

The combined visibility of the GNSS and SBAS systems is shown in Figure 10, which highlights that there is beyond doubt some benefit to be gained from using multiple GNSS constellations for relative positioning outside the GNSS service volumes. However, the GNSS signals present outside of the GNSS constellations are at the

threshold of detectability for a typical receiver, with the result that small changes in input conditions can have a fairly drastic impact on simulation results.

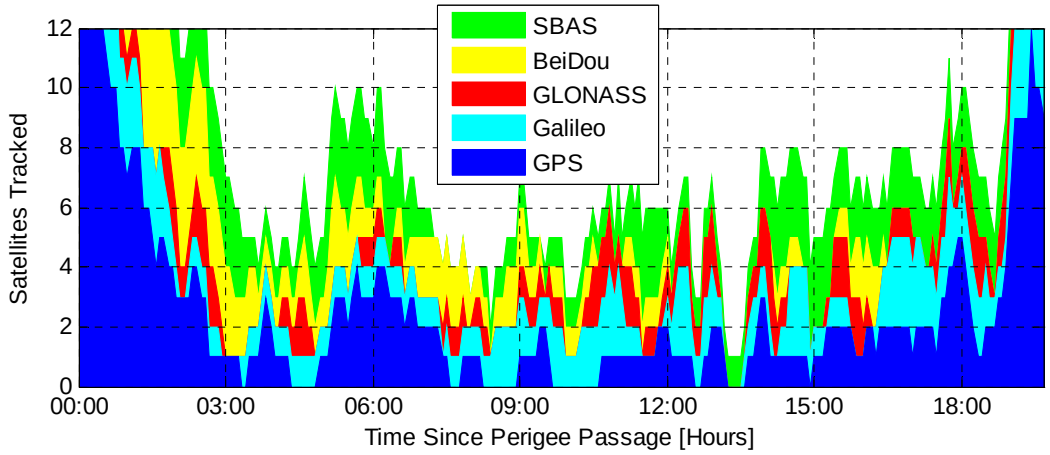


**Figure 10: Combined visibility for GPS, Galileo, GLONASS, QZSS, BeiDou, WAAS, EGNOS, GAGAN, SDCM and MSAS on the Proba-3 orbit**

It can be concluded that the availability of signals from any of the GNSS systems is highly dependent on mission parameters such as the alignment of the GNSS systems with the HEO orbital plane, the receiver antenna orientation, and the HEO orbital period with respect to the GNSS orbital periods. Other factors such as acquisition speed, the minimum required signal power for acquisition and the minimum required signal power for tracking are equally influential, and are dependent on the receiver design. Further, the visibility is strongly affected by factors such as the alignment of the GNSS systems with respect to each other, which evolves over time and will depend on the epoch of a future HEO formation flying mission, or the transmission gain patterns of the GNSS satellites, which have not been published on a sufficient level of detail for truly accurate results.

Because a small change in the mission design can potentially result in a drastic change in the availability of GNSS measurements, and because the unknown environmental factors have such a strong influence but cannot at present be accurately modeled, adapting the receiver design for weak signal tracking and optimal performance at HEO dynamics is also worth the investment.

## 5. Acknowledgments

The advice and guidance of my two academic advisors, Dr. Oliver Montenbruck and Dr. Kyle O'Keefe, is gratefully acknowledged. The financial support of both the Natural Sciences and Engineering Research Council of Canada (NSERC) and Alberta Innovates – Technology Futures (AITF) is likewise acknowledged.

## 6. References

[1] Kelbel, D., T. Lee, A. Long, R. Carpenter, and C. Gramling, "Relative Navigation Algorithms for Phase 1 of the MMS Formation," 2003, available at http://geons.gsfc.nasa.gov/library docs/.

[2] Bamford, W., Mitchell, J., Southward, M., Baldwin, P., Winternitz, L., Heckler, G., Kurichh, R., Sirotzky, S., "GPS Navigation for the Magnetospheric Multi-Scale Mission," Proceedings of the 22nd International Technical Meeting of The Satellite Division of the Institute of Navigation (ION GNSS 2009), Savannah, GA, September 2009, pp. 1447-1457.
[3] Mestreau-Garreau, A., K. Gantois, A. Santovincenzo, A. Cropp, D. Evans, M. François,P. Kerhousse and F. Teston, “PROBA 3 High Precision Formation Flying Mission” Proceedings of the Spacecraft Formation Flying Missions and Technologies conference, May 18-20, Montreal, Canada, 2011.
[4] Fernández Ibarz, J.M., L. Tarabini Castellani, M. Ruiz, J.S. Llorente, A. Mestreau-Garreau, K. Gantois and A. Cropp, “PROBA-3: Demonstrating Formation Flying,” Proceedings of the Spacecraft Formation Flying Missions and Technologies conference, May 18-20, Montreal, Canada, 2011.
[5] Dion, A., Calmettes, V., Boutillon, E., "Reconfigurable GPS-Galileo Receiver for Satellite Based Applications," Proceedings of ION GNSS 2007, Fort Worth, TX, September 2007, pp. 2448-2458.
[6] Lorga J.M., P.F. Silva, F. Dovis, A. Di Cintio, S. Kowaltschek, D. Jimenez, R. Jansson “Autonomous Orbit Determination for Future GEO and HEO Missions” Proceedings of NAVITEC, Noordwijk, the Netherlands, 8-10 December, 2010.
[7] Qiao, L., Lim, S., Rizos, C., Liu, J., "Autonomous GEO Satellite Navigation with Multiple GNSS Measurements," Proceedings of ION GNSS 2009, Savannah, GA, September 2009, pp. 2169-2177.
[8] Filippi, H. Gottzein, E. ; Kuehl, C. ; Mueller, C. ; Barrios-Montalvo, A. ; Dauphin, H. “Feasibility of GNSS receivers for satellite navigation in GEO and higher altitudes,” 5th ESA Workshop on Satellite Navigation Technologies and European Workshop on GNSS Signals and Signal Processing (NAVITEC), 8-10 Dec, Noordwijk, The Netherlands, 2010.
[9] Llorente J.S. Agenjo, A. Carrascosa, C. de Negueruela, C. Mesteau-Garreau, A., Cropp, A., Santovincenzo, A., “PROBA-3: Precise formation flying demonstration mission,” Acta Astronautica, Vol 82, No. 1, 2013, Pages 38–46.
[10] Ardaens, J. S., D’Amico, S., Cropp, A, “GPS-Based Relative Navigation for the Proba-3 Formation Flying Mission” 63rd International Astronautical Congress, Naples, Italy, 2012.
[11] GPS Wing, “Navstar GPS Space Segment / Navigation User Interfaces,” IS-GPS-200E, 8 June, 2010.
[12] Global Positioning System Directorate, “Navstar GPS Space Segment/User Segment L5 Interfaces,” IS-GPS-705B, 21 September 2011.
[13] Global Positioning System Directorate, “Navstar GPS Space Segment/User Segment L1C Interface,” IS-GPS-800B, 21 September 2011.
[14] Powell, T.D., P. D. Martzen, S.B. Sedlacek, C. Chao, R. Silva, A. Brown, G. Belle, “GPS Signals in a Geosynchronous Transfer Orbit: Falcon Gold Data Processing,” ION Nation Technical Meeting, January, 1999, pp. 575-585.
[15] Moreau, M., E.P. Davis, J.R. Carpenter, D. Kelbel, G.W. Davis, and P. Axelrad, “Results from the GPS Flight Experiment on the High Earth Orbit AMSAT OSCAR-40 Spacecraft,” ION GPS-2002, Portland, OR, September 2002, pp. 122-133.
[16] Ebinuma, T. and M. Unwin, “GPS Receiver Demonstration on a Galileo Test Bed Satellite,” the Journal of Navigation, Vol. 60, No. 3, 2007, 349–362. doi:10.1017/S0373463307004365
[17] Russian Institute of Space Device Engineering, “Global Navigation Satellite System Glonass Interface Control Document”, Edition 5.1, Moscow, 2008.
[18] Stupak, G., “GLONASS Status and Development Plans,” 5th Meeting of the International Committee on GNSS, Turin, Italy, 2010.
[19] Revnivykh, S. “GLONASS Status and Modernization,” 6th Meeting of the International Committee on GNSS, Tokyo, Japan, 2011.

[20] European Union, “European GNSS (Galileo) Open Service Signal in Space Interface Control Document,” OD-SIS-ICD Issue 1.1, September 2010.
[21] China Satellite Navigation Office, “BeiDou Navigation Satellite System Signal in Space Interface Control Document Open Service Signal B1I”, Version 1.0, December 2012.
[22] Hauschild, A., O. Montenbruck, J. M. Sleewaegen, L. Huisman, P. J. G. Teunissen “Characterization of Compass M1 Signals,” GPS Solutions, Vol. 16, 2012, pp. 117-126. DOI 10.1007/s10291-011-0210-3
[23] Montenbruck O., Hauschild A., Steigenberger P., Hugentobler U., Teunissen P., Nakamura S., “Initial Assessment of the COMPASS/BeiDou-2 Regional Navigation Satellite System,” GPS Solutions, Vol. 17, No. 2, 2013, pp. 211-222. DOI 10.1007/s10291-012-0272-x
[24] Japan Aerospace Exploration Agency, “Interface Specification for QZSS,” IS-QZSS V1.4, Feb 28, 2012.
[25] Kogure, S. “Program Update QZSS (Quasi-Zenith Satellite System),” ION GNSS 2012, Plenary Session Presentation, September 19, 2012.
[26] Federal Aviation Administration/Department of Transportation, “Global Positioning System Wide Area Augmentation System (WAAS) Performance Standard,” 1st Edition, USA, 31 October, 2008.
[27] European Commission, Directorate-General for Enterprise and Industry, “EGNOS Open Service Service Definition Document,” Version 2.0, 2013.
[28] Czopek, F. and S. Schollenberger, "Description and Performance of the GPS Block I and II L-Band Antenna and Link Budget," Proceedings of the Institute of Navigation GPS 93 Conference, 1993, pp. 37-43.
[29] Ericson, S. D., Shallberg, K. W., Edgar, C. E., "Characterization and Simulation of SVN49 (PRN01) Elevation Dependent Measurement Biases," Proceedings of the 2010 ION International Technical Meeting, San Diego, CA, 2010, pp. 963-974.
[30] Fisher ,S.C., Ghassemi, K., “GPS IIF—The Next Generation”, Proceedings of the IEEE, Vol. 87, No. 1, 1999, pp 24-47.
[31] Jyoti, R., Sanandiya, H. C., Kumar, S. S., Kumar, A. and S. B. Sharma, "Wideband Printed Helix Array Antenna at L1 & L5 for Navigaiton Satellite," Proceedings of the International Conference on Antenna Technologies, ICAT 2005, pp. 23-27.
[32] Montesano, A., C. Montesano, R. Caballero, M. Naranjo, F. Monjas, L. E. Cuesta, P. Zorrilla, L. Martinez, “Galileo System Navigation Antenna for Global Positioning,” 28th ESA Antenna Workshop on Space Antenna Systems and Technologies, Noordwijk, the Netherlands, May 31-June 3, 2005, pp. 247-252.
[33] Noda, H., Kogure, S., Kishimoto, M., Soga, H., Moriguchi, T. Furubayashi, T., “Development of the Quasi-Zenith Satellite System and High-Accuracy Positioning Experiment System Flight Model,” NEC Technical Journal, Vol. 5, No. 4, 2010, pp. 93-97.
[34] Iriarte, J. C., Ederra I., Gonzalo, R., Brand, Y., Fourmault, A., Demers, Y., Salgetti-Drioli, L., and de Maagt, P., “EBG Superstrate Array Configuration for the WAAS Space Segment,” IEEE Transactions on Antennas and Propagation, Vol. 57, No. 1, January 2009, pp. 81-93.
[35] Van Dierendonck, A.J. “GPS Receivers,” Chapter 8 in B. Parkinson et al. (editors), Global Positioning System: Theory and Applications, Vol. 1, Progress in Astronautics and Aeronautics, 1997.
[36] Lachapelle, G., “Advanced GNSS Theory and Applications,” ENGO 625 Course Notes, Geomatics Engineering Department, University of Calgary, 2009.
[37] M.Moreau, “GPS Receiver Architecture for Autonomous Navigation in High Earth Orbits,” Ph.D. Dissertation, Department of Aerospace Engineering Sciences, University of Colorado at Boulder, July 2001.
[38] Julien, O., “Carrier-Phase Tracking of Future Data/Pilot Signals,” Proceedings of ION GNSS 2005, Long Beach, CA, 13-16 September, 2005 pp. 113-124.